J. Chem. Eng. Data **1990**, *35*, 361–367

The Thermodynamics of "Scale" Mineral Solubilities. 3. Calcium Sulfate in Aqueous NaCl

Krishnam U. G. Raju and Gordon Atkinson*

Department of Chemistry, University of Oklahoma, Norman, Oklahoma 73019

Anhydrite and gypsum solubilities in water and aqueous NaCl are reviewed. The coefficients required to calculate $Cp°$, $\Delta H°$, $\Delta G°$, $\Delta S°$, and K_{sp} for the solubility equilibrium as a function of temperature are given. These thermodynamic quantities are calculated and compared with the available literature values. The transition temperature for the equilibrium between gypsum and anhydrite calculated by using these coefficients is 59.9 °C and is in agreement with the Hardie value of 58 ± 2 °C. Activity coefficients are calculated with a modified Pitzer formalism. A computer program is used to predict solubilities in NaCl solutions of anhydrite up to 250 °C and gypsum up to 110 °C.

Introduction

In continuation of our earlier work on alkaline-earth sulfate "scale" minerals (*1*, *2*), we now discuss $CaSO_4$ and $CaSO_4 \cdot 2H_2O$ solubilities in aqueous NaCl solutions.

In addition to the petroleum industry, all the industries that involve heating and cooling of water are concerned with scale problems. It is easier to remove calcium sulfate scale than barium and strontium sulfate scales. Because of the high concentrations of calcium ions in most reservoir brines and the high concentration of sulfate ions in the injection brines, commonly sea water, $CaSO_4$ scale is a common annoyance in "water flood" operations. Gypsum ($CaSO_4 \cdot 2H_2O$) is the most commonly occurring sulfate scale in the oil and gas industry. Gypsum forms at low temperatures whereas anhydrite ($CaSO_4$) forms at high temperatures. These two can be interconvertible under certain conditions. The transformation depends on conditions such as temperature, pressure, salinity, and the other ions present.

Literature

Anhydrite. A review of the literature on the solubilities of anhydrite and gypsum is given in Table I. Marshall and his associates (*16*) determined anhydrite solubility at 100–200 °C in synthetic sea salt solutions up to high ionic strengths. The saturation limits were estimated for saline waters in general. Templeton and Rodgers (*18*) ascribed the enhanced solubility in solutions of $CaCl_2$ and Na_2SO_4 between 250 and 325 °C to ionic strength effects and complex formation with sulfate ions. However, the K_{sp} values at these temperatures are lower than those of Marshall (*14*). Tsikaeva (*24*) observed a steep increase in solubility at approximately 93% H_2SO_4 and explained it as being due to the formation of the compound $CaSO_4 \cdot H_2SO_4$. Blount (*28*) studied the solubility in water and NaCl solutions at high temperatures and pressures. He observed that the solubility passes through a maximum with increasing NaCl concentration at temperatures up to ~175 °C, whereas at any given salinity the solubility passes through a minimum with increasing temperature.

There are many publications on the description of the solubility of anhydrite in NaCl–H_2O systems by empirical or quantitative relations. We propose the use of thermodynamic rela-

Table I. Review of Literature on the Solubilities of $CaSO_4$ (Anh) and $CaSO_4 \cdot 2H_2O$ (Gyp)

ref	sulfate species	experimental conditions
Melcher (*3*)	Anh	H_2O at 18, 50, 100, 156 and 218 °C
	Gyp	H_2O up to 100 °C
Hill (*4*)	Anh	H_2O at 42 °C
Booth (*5*)	Anh	H_2O between 141 and 408 °C
Partridge (*6*)	Anh	H_2O between 100 and 200 °C
Barton (*7*)	Anh	H_2O dissolution rates with Ca-ISE at 25 °C
Madgin (*8*)	Anh	H_2O between 20 and 35 °C
	Gyp	NaCl at 25 and 35 °C
Glater (*9*)	Anh	sea water up to 165 °C
Hill (*10–12*)	Anh	Na, K, and NH_4 sulfates at different temperatures
Tanaka (*13*)	Anh	sea water up to 200 °C
Marshall (*14a*)	Anh	H_2SO_4 between 25 and 350 °C
	Gyp	H_2SO_4 at 40 and 60 °C
Marshall (*14b*)	Gyp	NaCl between 125 and 200 °C
	Gyp	NaCl at 40 and 60 °C
Yeatts (*15*)	Ahn	Na_2SO_4 and $NaNO_3$ between 0 and 350 °C
Marshall (*16*)	Anh	sea salt between 100 and 200 °C
	Gyp	sea salt between 60 and 95 °C
Marshall (*17*)	Anh	$NaNO_3$ and $LiNO_3$ between 125 and 350 °C
Templeton (*18*)	Ahn	NaCl, $NaNO_3$, $CaCl_2$, $MgCl_2$, Na_2SO_4, and $Mg(NO_3)_2$ between 200 and 325 °C
Power (*19*)	Anh	H_2O and NaCl between 200 and 325 °C
	Gyp	H_2O and NaCl between 25 and 95 °C
Bock (*20*)	Anh and Gyp	NaCl between 25 and 50 °C
Posnjak (*21*)	Anh	sea salt at 30 °C
E-An-Zen (*22*)	Anh and Gyp	NaCl between 35 and 70 °C
Kruchenko (*23*)	Anh and Gyp	HNO_3 at 50 °C; $HClO_4$ between 25 and 50 °C
Tsikaeva (*24*)	Gyp	H_2SO_4 between 40 and 100 °C
Zdanovskii (*25*)	Anh	H_2SO_4 up to 50 °C
Glew (*26*)	Anh and Gyp	NaCl at 30 and 60 °C
Madgin (*27*)	Anh	NaCl at 25 °C
Blount (*28*)	Anh	H_2O and NaCl at high temperatures and high pressures
Hulett (*29*)	Gyp	H_2O up to 100 °C
Cameron (*30*)	Gyp	NaCl between 15 and 82 °C
Kruchenko (*32*)	Gyp	mineral acids and mixtures
Adler (*33*)	Gyp	natural and agriculture drinage waters at 25–70 °C
Shaffer (*34*)	Gyp	sea water up to 65 °C
Friedel (*36*)	Gyp	Na and Mg chlorides and sulfates at 25 °C
Ponizovskii (*37*)	Gyp	Ca–Mg–Na–Cl–SO_4–H_2O at 25 °C
Zdanovskii (*38*)	Gyp	$CaCl_2$ and $MgCl_2$ at 25 °C
Ostroff (*39*)	Gyp	NaCl–$MgCl_2$–H_2O between 28 and 70 °C
Marshall (*40*)	Gyp	NaCl between 0 and 110 °C
Yeats (*41*)	Gyp	Na_2SO_4–NaCl, Li_2SO_4–$LiNO_3$, and Li_2SO_4–LiCl at 25 °C
Barba (*42*)	Gyp	Na_2SO4–$MgCl_2$–H_2O at 40 °C
Tanji (*44*)	Gyp	Na, Ca, and Mg chlorides and sulfates at 25 °C

0021-9568/90/1735-0361$02.50/0

Table II. Coefficients of Thermodynamic Quantities for Species and Equilibria

$$C_p = A + BT + C/T_2$$
$$\Delta H° = AT + BT^2/2 - C/T + I_h$$
$$\Delta S° = A \ln T + BT - C/2T^2 + I_s$$
$$-\Delta G° = AT \ln T + BT^2/2 + C/2T - I_h - I_gT$$

	A	B	$10^{-6}C$	I_h	I_g	I_s
species						
SO_4^{2-}(aq)	818.323	-1.845 81	-49.7126	-1237 946	5762.58	-4371.65
Ca^{2+}(aq)	-58.534	0.0	4.6748	-509 536	-453.55	306.69
$CaSO_4$(s)	70.208	0.098 74	0.0	-1459 593	876.13	-322.75
$CaSO_4 \cdot 2H_2O$(s)	91.379	0.317 98	0.0	-2064 398	1461.01	-421.33
H_2O(l)	47.652	0.058 24	0.9188	-299 545	494.72	-213.80
equilibrium						
I	74.132	-0.102 76	-1.8376	5 715	404.59	-329.03
II	689.581	-1.944 55	-45.0378	-287 889	4432.90	-3742.21
III	763.714	-2.047 31	-43.2002	-282 176	4837.58	-4071.24

tionships to describe the solubility. Our purpose here is to describe the use of fundamental thermodynamic relations to calculate the thermodynamic solubility product and $\Delta H°$, $\Delta G°$, $\Delta S°$, and $\Delta C_p°$ of all the species and the equilibrium. The mean activity coefficients are calculated by the Pitzer (*43*) formalism with some modifications for mixing terms. Experimental solubility data published by different authors are used as our primary working tool for the calculations.

Gypsum. Marshall and his associates (*14*, *16*, *40*, *41*) studied the solubilities of gypsum in NaCl solutions up to saturation from 0 to 110 °C and in Na_2SO_4–NaCl, Li_2SO_4–LiCl, and Li_2SO_4–$LiNO_3$ systems at 25 °C. An extended Debye–Hückel equation with linear and quadratic ionic strength terms was used to calculate $\gamma_\pm$. From the calculated K_{sp} values, the thermodynamic parameters such as $\Delta H°$, $\Delta G°$, $\Delta S°$, and $\Delta C_p°$ were computed.

Some of the empirical or quantitative equations for the prediction of gypsum solubilities in the NaCl–H_2O system or in multicomponent systems are those of Tanji and Doneen (*44*) up to 0.04 M of NaCl, $MgCl_2$, and $MgSO_4$ at 25 °C; Skillman and his co-workers (*45*) in brines from 10 to 80 °C; Stiff and Davies (*31*) in Ca and Mg salts up to 100 °C. The most notable work in recent years is that of Harvie and Weare (*46*) in the Na–K–Mg–Ca–Cl–SO_4–H_2O system and Rogers (*47*) using the Pitzer formalism (*43*). They successfully reproduced the solubilities within experimental error but only at 25 °C. To apply the same technique at other temperatures, the Pitzer parameters, βs, ${}^S\theta$, and ψ, have to be known as a function of temperature. There are some reports (*48–50*) stating that ${}^S\theta$ and ψ are also functions of ionic strength. By considering them as $f(I,T)$, we successfully described the solubilities of barite (*1*) and celestite (*2*) in NaCl solutions at any given temperature.

The transition temperature between gypsum and anhydrite is also calculated from our thermodynamic coefficients.

Calculational Approach

Transition Temperature. The equilibrium between gypsum and anhydrite is

$$CaSO_4 \cdot 2H_2O(s) \rightleftharpoons CaSO_4(s) + 2H_2O(l) \qquad (I)$$

Hardie (*51*) has determined the transition temperature between gypsum and anhydrite equilibrium as a function of the activity of water in the solution and reported a value of 58 ± 2 °C. This value is slightly lower than that of Van't Hoff and co-workers (*52*), 60–66 °C, and significantly higher than the Posnjak (*21*) value of 42 ± 2 °C from solubility measurements. The near 42 °C value was supported by Partridge and White's (*6*) value of 38–39 °C; by Hill's (*4*) value of 42 ± 1 °C; by the value of Marshall and his associates of 42 °C; and by the thermodynamic data of Kelly and his co-workers (*53*), who calculated an equilibrium temperature of 40 °C. E-An Zen (*22*) pointed out that this value was obtained from inconsistant data and recalculated the transition temperature as 46 ± 25 °C. Ostroff (*54*) commented that gypsum will not be converted to anhydrite at temperatures below 97 °C in water. Innorta and his co-workers (*55*) obtained a transition temperature of 49.5 ± 2.5 °C. Blount and Dickson (*56*) argued that 40–42 °C was the minimum transition temperature and that no one has successfully reversed the solubility of anhydrite (precipitated it) below 70 °C. Their extrapolation of anhydrite solubility measurements from above 70 °C suggests an equilibrium temperature of 56 ± 3 °C, in good agreement with Hardie. Langmuir and Melchior (*57*) assumed that 56 °C was the correct transition temperature. From our thermodynamic coefficients, the transition temperature calculated is 59.9 °C, in good agreement with that of Hardie (*51*) and Blount and Dickson (*56*). This gives additional support to our approach in computing the thermodynamic solubility products from the thermodynamic coefficients of the species in the equilibrium. One of the differences between Kelly and co-workers and the present study is the thermodynamic coefficients used for H_2O(l). They expressed the C_p of H_2O(l) as independent of temperature and equal to 18.02 cal deg^{-1} mol^{-1}. We have taken the C_p of water at different temperatures from the NBS tables (*58*) and expressed it as a function of temperature as

$$C_p° = 47.652 + 0.05824T + 9.1881 \times 10^5/T^2 \qquad (1)$$

Hence the $\Delta G°$ for equilibrium I can be written as

$$\Delta G° = -74.132T \ln T + 0.10276T^2/2 - 18.376 \times 10^5/2T + 5715.34 + 404.59T \qquad (2)$$

This equation gives 333.05 K (59.9 °C) as the gypsum–anhydrite equilibrium temperature. This value is in good agreement with the value of Hardie (58 ± 2 °C), who presented unequivocal evidence of achieving the gypsum–anhydrite equilibrium. The coefficients and the integration constants for the species present in the equilibrium are given in Table II, and the thermodynamic parameters for this equilibrium are given in Table III. The transition temperature decreases with increasing NaCl concentration in the solution. MacDonald (*59*) expressed it as a function of NaCl concentration.

Anhydrite. The solubility equilibrium for $CaSO_4$(s) is

$$CaSO_4(s) \rightleftharpoons Ca^{2+}(aq) + SO_4^{2-}(aq) \qquad (II)$$

The thermodynamic solubility product is given by

$$K_{sp} = a_{Ca^{2+}(aq)} a_{SO_4^{2-}(aq)} \qquad (3)$$

and for pure $CaSO_4$ dissolving

$$K_{sp} = s^2 \gamma_\pm^2 \qquad (4)$$

where s is the solubility in moles/kg of H_2O and $\gamma_\pm$ is the mean activity coefficient. We have chosen to use the most consistent

Table III. Thermodynamic Quantities at Different Temperatures for the Species

T/°C	$\Delta H°$/ (kJ mol^{-1})	$\Delta G°$/ (kJ mol^{-1})	$\Delta S°$/(J K^{-1} mol^{-1})	$\Delta C_p°$/(J K^{-1} mol^{-1})
SO_4^{2-}(aq)				
0.0	-901.28	-758.02	48.1	-352.2
25.0	-909.27	-744.54	20.1	-291.2
50.0	-916.04	-730.45	-1.7	-254.2
75.0	-922.12	-715.86	-19.9	-234.4
100.0	-927.87	-700.84	-35.8	-227.5
125.0	-933.57	-685.44	-50.6	-230.2
150.0	-939.44	-669.68	-64.9	-240.4
175.0	-945.64	-653.57	-79.1	-256.4
200.0	-952.30	-637.10	-93.6	-277.1
225.0	-959.53	-620.26	-108.5	-301.5
250.0	-967.40	-603.04	-123.9	-329.0
275.0	-975.99	-585.43	-139.9	-358.9
300.0	-985.36	-567.41	-156.6	-390.9
Ca^{2+}(aq)				
0.0	-542.64	-552.28	-53.0	-4.1
25.0	-542.67	-553.17	-53.1	-5.9
50.0	-542.92	-554.04	-53.9	-13.8
75.0	-543.34	-554.88	-55.2	-20.0
100.0	-543.91	-555.69	-56.7	-25.0
125.0	-544.58	-556.46	-58.5	-29.0
150.0	-545.35	-557.18	-60.4	-32.4
175.0	-546.20	-557.86	-62.3	-35.3
200.0	-547.11	-558.48	-64.3	-37.7
225.0	-548.08	-559.06	-66.3	-39.7
250.0	-549.09	-559.59	-68.3	-41.5
275.0	-550.15	-560.06	-70.2	-43.0
300.0	-551.24	-560.49	-72.2	-44.3
H_2O(l)				
0.0	-287.72	-241.29	63.3	75.87
10.0	-286.96	-239.60	66.0	75.60
20.0	-286.21	-237.94	68.6	75.42
25.0	-285.83	-237.12	69.9	75.35
30.0	-285.45	-236.31	71.1	75.31
40.0	-284.70	-234.70	73.6	75.26
50.0	-283.95	-233.12	76.0	75.27
60.0	-283.20	-231.55	78.3	75.33
70.0	-282.44	-230.01	80.5	75.44
80.0	-281.69	-228.50	82.6	75.59
90.0	-280.93	-227.00	84.8	75.77
100.0	-280.17	-225.53	86.8	75.98
110.0	-279.41	-224.07	88.8	76.23
120.0	-278.65	-222.64	90.8	76.49
$CaSO_4$(s)				
0.0	-1436.73	-1331.55	98.1	97.2
25.0	-1434.27	-1322.03	106.7	99.6
50.0	-1431.75	-1312.72	114.8	102.1
75.0	-1429.17	-1303.61	122.5	104.6
100.0	-1426.52	-1294.68	129.9	107.1
125.0	-1423.81	-1285.94	136.9	109.5
150.0	-1421.04	-1277.37	143.6	112.0
175.0	-1418.21	-1268.96	150.1	114.5
200.0	-1415.32	-1260.71	156.4	116.9
225.0	-1412.37	-1252.62	162.5	119.4
250.0	-1409.35	-1244.68	168.4	121.9
275.0	-1406.27	-1236.88	174.1	124.3
300.0	-1403.13	-1229.22	179.7	126.8
$CaSO_4 \cdot 2H_2O$(s)				
0.0	-2027.58	-1817.21	178.2	178.2
10.0	-2025.78	-1809.54	184.6	181.4
20.0	-2023.95	-1801.94	191.0	184.6
25.0	-2023.02	-1798.16	194.1	186.2
30.0	-2022.09	-1794.40	197.2	187.8
40.0	-2020.19	-1786.92	203.4	191.0
50.0	-2018.27	-1779.50	209.4	194.1
60.0	-2016.31	-1772.14	215.4	197.3
70.0	-2014.32	-1764.84	221.3	200.5
80.0	-2012.30	-1757.60	227.1	203.7
90.0	-2010.25	-1750.41	232.8	206.9
100.0	-2008.16	-1743.29	238.5	210.0
110.0	-2006.05	-1736.22	244.1	213.2
120.0	-2003.90	-1729.20	249.6	216.4

Table IV. Thermodynamic Quantities at Different Temperatures for the Equilibria

T/°C	$\Delta H°$/ (kJ mol^{-1})	$\Delta G°$/ (kJ mol^{-1})	$\Delta S°$/(J K^{-1} mol^{-1})	$\Delta C_p°$/(J K^{-1} mol^{-1})
$CaSO_4 \cdot 2H_2O(s) \rightleftharpoons CaSO_4(s) + 2H_2O(l)$				
0.0	15.40	3.10	46.5	70.7
10.0	16.10	2.64	49.0	68.0
20.0	16.76	2.15	51.3	65.4
25.0	17.09	1.90	52.4	64.2
30.0	17.40	1.64	53.4	63.0
40.0	18.02	1.11	55.4	60.7
50.0	18.62	0.56	57.3	58.5
55.0	18.91	0.28	58.2	57.5
59.9	19.19	0.00	59.0	56.5
65.0	19.47	-0.30	59.9	55.5
70.0	19.75	-0.59	60.7	54.5
80.0	20.28	-1.19	62.2	52.6
90.0	20.80	-1.80	63.7	50.7
100.0	21.29	-2.44	65.0	49.0
110.0	21.78	-3.08	66.3	47.3
120.0	22.24	-3.73	67.5	45.6
$CaSO_4(s) \rightleftharpoons Ca^{2+}(aq) + SO_4^{2-}(aq)$				
0.0	-7.19	21.24	-103.0	-445.2
25.0	-17.66	24.32	-139.7	-396.8
50.0	-27.21	28.24	-170.5	-370.1
75.0	-36.30	32.87	-197.6	-359.0
100.0	-45.26	38.15	-222.4	-359.5
125.0	-54.34	44.03	-246.0	-368.7
150.0	-63.75	50.50	-268.9	-384.8
175.0	-73.63	57.53	-291.6	-406.1
200.0	-84.09	65.13	-314.3	-431.7
225.0	-95.24	73.30	-337.2	-460.6
250.0	-107.14	82.05	-360.5	-492.3
275.0	-119.87	91.40	-384.3	-526.2
300.0	-133.47	101.33	-408.5	-562.0
$CaSO_4 \cdot 2H_2O(s) \rightleftharpoons Ca^{2+}(aq) + SO_4^{2-}(aq) + 2H_2O(l)$				
0.0	8.21	24.37	-56.5	-374.5
10.0	4.57	25.02	-69.6	-354.8
20.0	1.10	25.81	-81.6	-339.2
25.0	-0.58	26.24	-89.3	-332.7
30.0	-2.23	26.71	-92.8	-327.0
40.0	-5.45	27.71	-103.3	-317.9
50.0	-8.59	28.82	-113.2	-311.6
60.0	-11.69	30.03	-122.6	-307.6
70.0	-14.75	31.33	-131.7	-305.7
80.0	-17.81	32.71	-140.4	-305.7
90.0	-20.87	34.19	-149.0	-307.3
100.0	-23.96	35.74	-157.4	-310.5
110.0	-27.09	37.39	-165.6	-315.0
120.0	-30.26	39.11	-173.8	-320.7

literature solubility data as our basic working tool. Details of the calculational approach and the equations for $C_p°$, $\Delta H°$, $\Delta G°$, and $\Delta S°$ and ln K_{sp} for the $CaSO_4$ system are the same as we used for $BaSO_4$ and $SrSO_4$ (*1*, *2*). Here we give the ln K_{sp} equation as a quick reference:

$$\ln K_{sp} = A \ln T/R + BT/2R + C/2RT^2 - I_h/RT - I_g/R \tag{5}$$

The coefficients for different species and for the equilibrium are given in Table II. The $C_p°$, $\Delta H°$, $\Delta G°$, and $\Delta S°$ values at different temperatures for Ca^{2+}, SO_4^{2-}, and $CaSO_4$(s) are given in Table III. These thermodynamic quantities and K_{sp} for the equilibrium are reported in Tables IV and V, respectively, along with other available K_{sp} values and are plotted against temperature in Figure 1. There are differences among the Marshall values published at different times. Helgeson's (*60*) values are lower than ours at lower temperatures but in agreement with our values at higher temperatures. The Khodakovskiy (*61*) data and the Templeton and Rodger (*18*) data deviate at higher temperatures. Recently, Langmuir and Melchior (*57*) studied the geochemistry of Ca, Sr, Ba, and Ra sulfates in some deep

Table V. Comparison of –log K_{sp} for Anhydrite with Literature Values at Different Temperatures

							ref 57	
T/°C	this work	ref 61	ref 60	ref 14b	ref 15	ref 16	a	b
0.0	4.066	3.99			3.907	3.818	3.98	4.09
25.0	4.265	4.23	4.70	4.201	4.267	4.192	4.24	4.28
40.0	4.437			4.321			4.42	4.44
50.0	4.568	4.52	4.99		4.623	4.539	4.56	4.56
60.0	4.709			4.542			4.69	4.70
75.0	4.935	4.84	5.09			4.884	4.90	4.92
100.0	5.344	5.19	5.63	5.112	5.362	5.240	5.28	5.32
125.0	5.781	5.56		5.648		5.617	5.66	5.76
150.0	6.238	5.96	6.35	6.000	6.173	6.020	6.05	6.22
175.0	6.710	6.36		6.474		6.453	6.45	6.70
200.0	7.195	6.79	7.18	6.943	7.072	6.917	6.84	7.18
225.0	7.690	7.22					7.24	7.67
250.0	8.197	7.66	8.12		8.061	7.941	7.63	8.16
275.0	8.713	8.11					8.01	8.65
300.0	9.239	8.58	9.05		9.138	9.093	8.40	9.13

Table VI. Comparison of –log K_{sp} for Gypsum with Literature Values at Different Temperatures

T/°C	this work	ref 40	ref 57	ref 66	ref 19	ref 70	ref 54
0.0	4.659	4.465	4.617				
0.5	4.656	4.462	4.615	4.662			
10.0	4.616	4.408	4.591				
20.0	4.598	4.378	4.581				
25.0	4.597	4.373	4.581	4.598	4.359	4.367	
28.0	4.599	4.371	4.582				4.345
30.0	4.601	4.372	4.584				
35.0	4.610	4.375	4.589		4.370		
38.0	4.617	4.379	4.594				4.326
40.0	4.622	4.383	4.600			4.377	
45.0	4.639	4.394	4.608		4.396		
50.0	4.659	4.408	4.621				4.364
60.0	4.708	4.444	4.654			4.439	
65.0	4.737	4.466	4.673		4.461		
70.0	4.768	4.489	4.694				4.439
80.0	4.838	4.539	4.741			4.532	
85.0	4.877	4.566	4.767		4.559		
90.0	4.917	4.593	4.794				4.511
95.0	4.959	4.621	4.822		4.614		
100.0	5.003	4.650	4.852			4.622	
110.0	5.096	4.707	4.914				
120.0	5.196	4.763	4.981				

Table VII. Sources for Pitzer Coefficients

system	at 25 °C	ref	at other temp	ref
Ca-SO_4	SO_4 model	47	$MgSO_4$ model	62
Ca-Cl	$CaCl_2$ actual	47	$CaCl_2$ model	63
Na-SO_4	Na_2SO_4 actual	64	Na_2SO_4 actual	64
Na-Cl	NaCl actual	65	NaCl actual	65

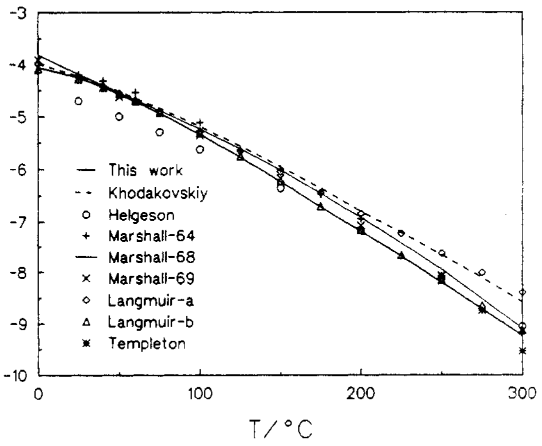

Figure 1. log K_{sp} vs T/°C for anhydrite.

brines from the Palo Duro Basin, TX. They reported the K_{sp} values as a function of temperature by (a) modeling Blount and Dickson's data (*56*) and by (b) taking an independent approach based on the thermodynamics. Our present values are in good agreement with their values and those of Marshall (*15*) up to 200 °C. But the K_{sp} values decrease continuously with temperature—the same trend observed by others.

The treatment for the calculation of the mean activity coefficients of $CaSO_4$ is the same as that for $BaSO_4$, which we described in our earlier paper (*1*). Hence, only the final equation is given here as

$$\begin{aligned}\ln \gamma_{\pm} = {} & 4f^{\gamma} + m_{M}(2B_{MS} + 2EC_{MS}) + \\ & m_{N}(B_{MC} + B_{NS} + E(C_{MC} + C_{NS})) + \\ & m_{M}^{2}(4B'_{MS} + 2C_{MS}) + m_{M}m_{N}(4B'_{MC} + 4B'_{NS} + 2C_{MC} + \\ & 2C_{NS}) + m_{N}^{2}(4B'_{NC} + 2C_{NC}) + m_{N}({}^{E}\theta_{MN} + {}^{E}\theta_{SC}) + \\ & 4m_{M}m_{N}(\theta'_{MN} + \theta'_{SC}) + m_{N}({}^{S}\theta_{MN} + {}^{S}\theta_{SC}) + \\ & m_{M}m_{N}(\psi_{MNS} + \psi_{MSC}) + m_{N}^{2}(\psi_{MNC} + \psi_{NSC})/2 \end{aligned} \quad (6)$$

where the subscripts M, N, S, and C refers to Ca^{2+}, Na^{+}, SO_4^{2-}, and Cl^{-} ions, respectively, and all other terms have their usual significance. The Pitzer coefficients, $\beta^{(0)}$, $\beta^{(1)}$, and $\beta^{(2)}$, for $CaSO_4$ at temperatures other than 25 °C can be calculated from the equation

$$\beta^{(i)} = a + b(T - Tr) + c(T^2 - Tr^2) \quad (7)$$

by setting $a = \beta^{(i)}$ of $CaSO_4$ at 25 °C and assuming that the b and c values are the same as the parameters reported for $MgSO_4$ by Holmes and Mesmer (*62*). In the absence of the actual temperature dependence of the Pitzer coefficients for calcium, strontium, and barium sulfates, we have modeled them

Table VIII. Coefficients for $CaSO_4$ and $CaCl_2$ in the Equation for $\beta^{(i)}$ or C^{ϕ}

$$\beta^{(i)} \text{ or } C^{\phi} = a + b(T - Tr) + c(T^2 - Tr^2) + d(1/T - 1/Tr) + e \ln (T/Tr)$$

salt	function	a	b	c	d	e
$CaSO_4$	$\beta^{(0)}$	0.200 00	0.002 916	-3.872×10^{-6}	0	0
	$\beta^{(1)}$	3.1973	0.001 24	1.809×10^{-5}	0	0
	$\beta^{(2)}$	-54.24	0.8283	-0.001 782	0	0
$CaCl_2$	$\beta^{(0)}$	0.3397	-0.1390	6.286×10^{-5}	5108.0	46.48
	$\beta^{(1)}$	1.5050	-0.016 47	2.346×10^{-1}	498.24	0.0
	C^{ϕ}	-0.026 79	0.2462	-1.184×10^{-4}	-9676.3	-84.83

Table IX. Coefficients in Equations 8 and 14

	anhydrite	gypsum
B_1	$-3.736 64 \times 10^3$	-82.6504
B_2	$4.028 91 \times 10^3$	109.860
B_3	$-1.275 89 \times 10^3$	-36.2700
B_4	31.4958	0.548 561
B_5	-33.5633	-0.741 554
B_6	10.6681	0.256 380
B_7	-0.087 0369	$-9.308 22 \times 10^{-4}$
B_8	0.091 3125	$1.257 69 \times 10^{-3}$
B_9	-0.029 0883	$-4.383 26 \times 10^{-4}$
B_{10}	$7.895 91 \times 10^{-5}$	0.0
B_{11}	$-8.115 00 \times 10^{-5}$	0.0
B_{12}	$2.593 49 \times 10^{-5}$	0.0

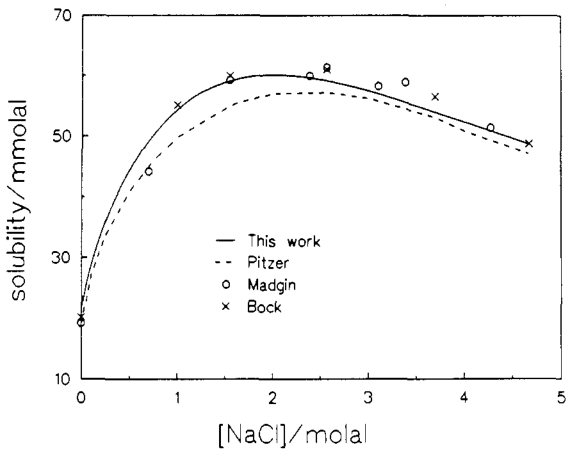

Figure 2. Calculated and experimental solubility vs m_{NaCl} at 25 °C for anhydrite.

as magnesium sulfate because of similar chemistry of the alkaline-earth sulfates in aqueous systems. We use the coefficient sources given in Table VII. The coefficients for $CaSO_4$ and $CaCl_2$ are given in Table VIII. The γ_{calc} is given by the equation

$$\ln \gamma_{calc} = \ln \gamma^* + m_M[(B_1 + B_2 I^{1/2} + B_3 I) + (B_4 + B_5 I^{1/2} + B_6 I)T + (B_7 + B_8 I^{1/2} + B_9 I)T^2 + (B_{10} + B_{11} I^{1/2} + B_{12} I)T^3] \quad (8)$$

where γ^* is calculated from eq 6 without the ${}^S\theta$ and ψ parameters, which we believe are dependent on ionic strength. The coefficients are given in Table IX. The sequence of analysis and the flow chart of the program are the same as that for $BaSO_4$ (*1*).

The $\gamma_\pm$ values were calculated using the Pitzer formalism with ${}^S\theta$ and ψ values at 25 °C and K_{sp} obtained is 3.70×10^{-5}. The K_{sp} value was calculated for the Bock solubility data in NaCl solutions at 25 °C, varying from 2.96×10^{-5} to 4.14×10^{-5} with an average value of 3.70×10^{-5}. A value of 5.435×10^{-5} was reported by Langmuir and Melchior, Marshall, and Khodakovskiy. If this K_{sp} value were considered to be correct, some corrections have to be made to the equation or the ${}^S\theta$ and ψ values have to be redetermined.

Solubility Check for Anhydrite. The predicted solubility of anhydrite is plotted against the molality of NaCl at 25 °C in Figure 2 and at 100, 150, and 200 °C in Figure 3 along with

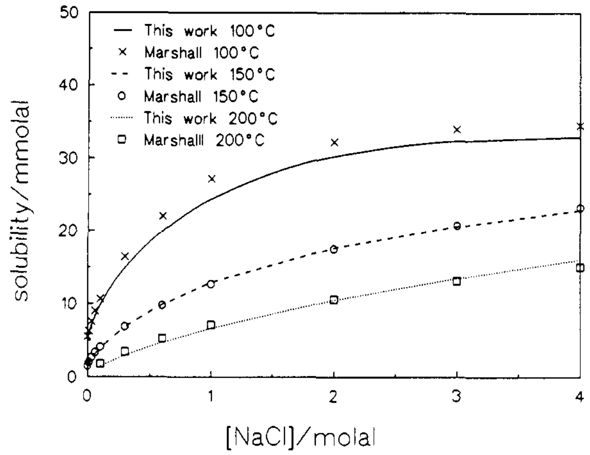

Figure 3. Calculated and experimental solubility vs m_{NaCl} at higher temperatures for anhydrite.

Marshall's (*16*) experimental values. Marshall's calculated values with Debye–Hückel parameters and with their calculated K_{sp} values are also in good agreement with the experimental values. Predicted values from the Pitzer formalism at 25 °C with $K_{sp} = 3.70 \times 10^{-5}$ are also plotted in Figure 2 for comparison. If we consider ${}^S\theta$ and ψ as independent of ionic strength, then the curve with $K_{sp} = 3.70 \times 10^{-5}$ agrees with the experimental values. Our predicted values are in excellent agreement with literature values at all concentrations of NaCl.

Gypsum. The dissolution equilibrium for gypsum in aqueous solutions is

$$CaSO_4 \cdot 2H_2O(s) \rightleftharpoons Ca^{2+}(aq) + SO_4^{2-}(aq) + 2H_2O(l) \quad (III)$$

The thermodynamic solubility product is given by

$$K_{sp} = a_{Ca^{2+}(aq)} a_{SO_4^{2-}(aq)} a_{H_2O}^2 \quad (9)$$

and for pure gypsum dissolving

$$K_{sp} = s^2 \gamma_\pm^2 a_{H_2O}^2 \quad (10)$$

where s is the solubility in moles/kg of H_2O, $\gamma_\pm$ is the mean activity coefficient, and a_{H_2O} is the activity of water. Emphasis must be given to the fact that s is the experimental fact and $\gamma_\pm$ is the calculated value depending on the model chosen for it in computing the literature K_{sp} values. Rogers (*47*), Culberson and co-workers (*66*), and Krumgalz and Millero (*67*) reported the K_{sp} value to be 2.532×10^{-5} at 25 °C by calculating the a_{H_2O} and $\gamma_\pm$ by the Pitzer formalism. Lilley and Briggs (*68*) calcualted the K_{sp} value to be 2.63×10^{-5} from emf measurements. The Nakayama and Rasniks's (*69*) extrapolated value from emf studies was 2.50×10^{-5}. Power (*19*) neglected the a_{H_2O} and reported the value to be 4.38×10^{-5}. Lu and Fabuss (*70*) reported the K_{sp} value as 4.30×10^{-5}, whereas Marshall and his associates (*14*, *16*, *41*) used the extended Debye–Hückel equation with linear and quadratic ionic strength terms to calculate $\gamma_\pm$. They assumed that these terms accounted for a_{H_2O} and reported the K_{sp} value as 4.231×10^{-5} (*41*), 4.22×10^{-5} (*14*) and 4.236×10^{-5} (*16*). Hence, these K_{sp} values are not independent of the assumptions made about $\gamma_\pm$ and a_{H_2O}.

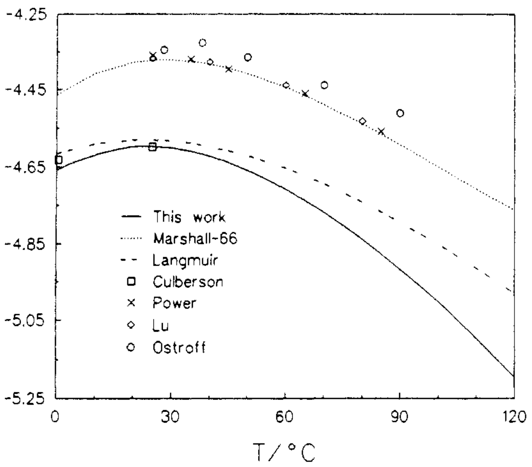

Figure 4. log K_{sp} vs $T/°C$ for gypsum.

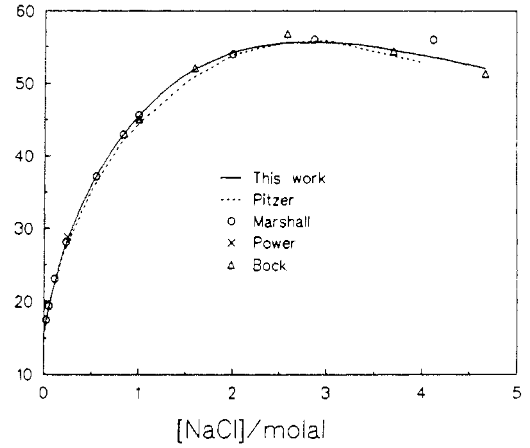

Figure 5. Calculated and experimental solubility vs m_{NaCl} at 25 °C for gypsum.

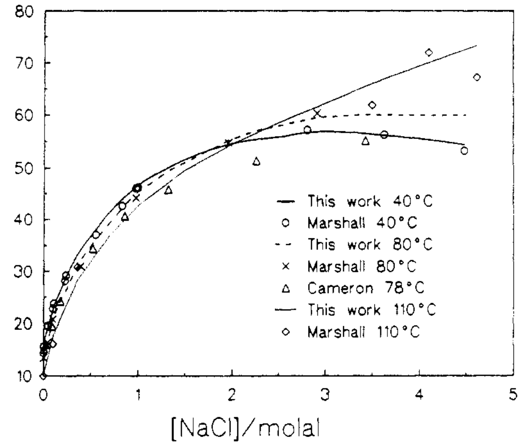

Figure 6. Calculated and experimental solubility vs m_{NaCl} at higher temperatures for gypsum.

The details of the calculations were discussed earlier (*1*, *2*). The coefficients are given in Table II, and the $C_p°$, $\Delta H°$, $\Delta G°$, and $\Delta S°$ values at different temperatures for $H_2O(l)$ and $CaSO_4{\cdot}2H_2O(s)$ are given in Table III. These thermodynamic quantities and K_{sp} for the equilibrium are given in Tables IV and VI, respectively, along with other literature values for comparison. The log K_{sp} values are plotted against temperature in Figure 4. Our values at 25 °C are in good agreement with Culberson (*66*), Rogers (*50*), and Krumgalz (*67*) values. Our K_{sp} values up to 110 °C are closer to Langmuir and Melchior's (*57*) values within 0.1 log unit, whereas the Marshall and co-workers (*14*, *16*, *41*), Power (*19*), and Lu and Ostroff (*70*) values deviate by about 0.2 log unit. We fixed the I_h and I_g coefficient values by taking Culberson, Rogers, and Krumgalz K_{sp} values as being correct at 25 °C.

The calculational approach for the activity coefficients of gypsum using the Pitzer formalism is almost same as that for anhydrite. The only difference between gypsum and other sulfates is the term a_{H_2O}. This can be written as

$$Y = \gamma_{\pm} a_{H_2O} \tag{11}$$

$$= \gamma_{\pm} f'(I,T) a_{H_2O} \tag{12}$$

On futher simplification, this gives

$$Y = \gamma^{*} f(I,T) \tag{13}$$

and the treatment is the same as for anhydrite. Now a_{H_2O} is included in $f(I,T)$ where

$$f(I,T) = m_M[(B_1 + B_2 I^{1/2} + B_3 I) + (B_4 + B_5 I^{1/2} + B_6 I)T + (B_7 + B_8 I^{1/2} + B_9 I)T^2] \tag{14}$$

where m_M is the concentration of Ca^{2+} ion and nine coefficients are sufficient to reproduce the experimental solubilities.

Solubility Check for Gypsum. The predicted solubility of gypsum against NaCl concentration is plotted at 25 °C in Figure 5 along with the experimental values. The predicted values of Rogers (*47*) using the Pitzer formalism at 25 °C are also plotted for comparison, and they are in good agreement. At all temperatures our predicted solubilities are in excellent agreement with the literature values at all concentrations of NaCl, as shown in Figure 6. The gypsum solubility does not change with temperature for NaCl concentrations up to 2.5 *m*. The average deviation for the Marshall and Slusher data from 0 to 110 °C (98 points) is only 1.53%, for the Marshall and co-workers data (14 points) is 1.04%, for the Power data (18 points) is 1.4%, for the Ostroff and Metler data (46 points) is 2.67%, for the Bock data (24 points) is 2.85%, and for the Cameron data (31 points) is 4.43%.

Literature Cited

(1) Raju, U. G. K.; Atkinson, G. *J. Chem. Eng. Data* **1988**, *33*, 490.
(2) Raju, U. G. K.; Atkinson, G. *J. Chem. Eng. Data* **1989**, *34*, 361.
(3) Melcher, A. C. *J. Am. Chem. Soc.* **1910**, *32*, 50.
(4) Hill, A. E. *J. Am. Chem. Soc.* **1937**, *59*, 2242.
(5) Booth, H. S.; Bidwell, R. M. *J. Am. Chem. Soc.* **1950**, *72*, 2567.
(6) Partridge, E. P.; White, A. H. *J. Am. Chem. Soc.* **1929**, *51*, 360.
(7) Barton, A. F. M.; Wilde, N. M. *Trans. Faraday Soc.* **1971**, *67*, 3590.
(8) Madgin, W. M.; Swales, D. A. *J. Chem. Soc.* **1956**, *159*, 196.
(9) Glater, J.; Schwartz, J. *J. Chem. Eng. Data* **1976**, *21*, 47.
(10) Hill, A. E. *J. Am. Chem. Soc.* **1934**, *56*, 1071.
(11) Hill, A. E.; Yanic, N. S. *J. Am. Chem. Soc.* **1935**, *57*, 645.
(12) Hill, A. E.; Wills, J. H. *J. Am. Chem. Soc.* **1938**, *60*, 1647.
(13) Tanaka, Y.; Nakamura, K.; Hara, R. *J. Soc. Chem. Ind. Jpn.* **1931**, *34*, 284.
(14) (a) Marshall, W. L.; Jones, E. V. *J. Phys. Chem.* **1966**, *70*, 4028. (b) Marshall, W. L.; slusher, R.; Jones, E. V. *J. Chem. Eng. Data* **1964**, *9*, 187.
(15) Yeatts, L. B.; Marshall, W. L. *J. Phys. Chem.* **1969**, *73*, 81.
(16) Marshall, W. L.; Slusher, R. *J. Chem. Eng. Data* **1968**, *13*, 83.
(17) Marshall, W. L.; Slusher, R. *J. Chem. Thermodyn.* **1973**, *5*, 189.
(18) Templeton, C. C.; Rodgers, J. C. *J. Chem. Eng. Data* **1967**, *12*, 536.
(19) Power, W. H.; Fabuss, B. M.; Satterfield, C. N. *J. Chem. Eng. Data* **1966**, *11*, 149.
(20) Bock, E. *Can. J. Chem.* **1961**, *39*, 1746.
(21) Posnjak, E. *Am. J. Sci.* **1940**, *238*, 559.
(22) Zen, E-An. *J. Petrol.* **1965**, *6*, 124.
(23) Kruchenko, V. P.; Beremzhanov, B. A. *Zn. Neorg. Khim.* **1978**, *23*, 210, 1922.
(24) Tsikaeva, D. V. *Zh. Neorg. Khim.* **1980**, *25*, 3073.
(25) Zdanovskii, A. B.; Vlasov, G. A. *Zh. Neorg. Khim.* **1968**, *13*, 2552.
(26) Glew, D. N.; Hames, D. A. *Can. J. Chem.* **1970**, *48*, 3733.
(27) Madgin, W. M.; Swales, D. A. *J. Appl. Chem.* **1956**, *6*, 482.
(28) Blount, C. W. Ph.D. Thesis, University of California, Los Angeles, 1965.
(29) Hulett, G. A.; Allen, L. E. *J. Am. Chem. Soc.* **1902**, *24*, 667.
(30) Cameron, F. K. *J. Phys. Chem.* **1901**, *5*, 556.
(31) Stiff, H. A.; Davies, L. F. *J. Pet. Technol.* **1952**, *4*, 25.
(32) Kruchenko, V. P.; Beremzhanov, B. A. *Zn. Neorg. Khim.* **1975**, *20*, 3153; **1980**, *25*, 3076; **1982**, *27*, 2415; **1983**, *28*, 242.
(33) Adler, M. S.; Glater, J.; McCutchan, J. W. *J. Chem. Eng. Data* **1979**, *24*, 187.

(34) Shaffer, L. H. *J. Chem. Eng. Data* **1967**, *12*, 183.
(35) Tanji, K. *Environ. Sci. Technol.* **1969**, *3*, 656.
(36) Friedel, V. B. *Z. Pflanzenernaehr. Bodenkd.* **1978**, *141*, 337.
(37) Ponizovskii, A. A.; Pachenskii, Ya. A. *Zh. Neorg. Khim.* **1979**, *24*, 161.
(38) Zdanovskii, A. B.; Chernova, Z. S. *Zh. Neorg. Khim.* **1976**, *20*, 2578.
(39) Ostroff, A. G.; Metler, A. V. *J. Chem. Eng. Data* **1966**, *11*, 346.
(40) Marshall, W. L.; Slusher, R. *J. Phys. Chem.* **1966**, *70*, 4015.
(41) Yeatts, L. B.; Marshall, W. L. *J. Chem. Eng. Data* **1972**, *17*, 163.
(42) Barba, D.; Brandani, V.; Giacomo, G. Di. *J. Chem. Eng. Data* **1984**, *29*, 42.
(43) Pitzer, K. S. In *Activity coefficients in electrolyte solutions*; Pytkowicz, R. M., Ed.; *CRC Press*, Boca Raton, FL, 1979; Vol. 1, Chapter 7.
(44) Tanji, K. K.; Doneen, L. D. *Water Resour. Res.* **1966**, *2*, 543.
(45) Skillman, H. L.; McDonald, J. P., Jr.; Stiff, H. A., Jr. Presented at the Spring Meeting of Southwestern District Division of Production, March 12–14, 1969.
(46) Harvie, C. E. Weare, J. H. *Geochim. Cosmochim. Acta* **1980**, *44*, 981.
(47) Rogers, P. S. Z. Ph.D. Thesis, University of California, Berkely, CA, 1980.
(48) Ananthaswamy, J.; Atkinson, G. *J. Solution Chem.* **1982**, *11*, 509.
(49) Hanna, T. M.; Atkinson, G. *J. Phys. Chem.* **1985**, *89*, 4884.
(50) Usha, A. V.; Raju, U. G. K.; Atkinson, G. *J. Phys. Chem.* **1987**, *91*, 4796.
(51) Hardie, L. A. *Am. Mineral.* **1967**, *52*, 171.
(52) Van't Hoff, J. H.; Armstrong, E. F.; Henrichsen, W.; Weigert, F.; Just, G. *Z. Phys. Chem.* **1903**, *45*, 257.
(53) Kelly, K. K.; Southard, J. C.; Anderson, C. T. *U.S. Bur. Mines Technol. Paper* 1941, *625*.
(54) Ostroff, A. G. *Geochim. Cosmochim. Acta* **1964**, *28*, 1363.
(55) Innorta, G.; Rabbi, E.; Toamdin, L. *Geochim. Cosmochim. Acta* **1980**, *44*, 1931.
(56) Blount, C. W.; Dickson, F. W. *Am. Mineral.* **1973**, *58*, 323.
(57) Langmuir, D.; Melchior, D. *Geochim. Cosmochim. Acta* **1985**, *49*, 2423.
(58) Parker, V. B.; Wagman, D. D.; Evans, W. H. *NBS Tech. Note* **1971**, *No. 276-6*.
(59) MacDonald, G. J. F. *Am. J. Sci.* **1953**, *251*, 884.
(60) Helgeson, H. C. *Am. J. Sci.* **1969**, *267*, 729.
(61) Khodakovskiy, I. L.; Mishin, I. V.; Zhogina, V. V. *Geokhimiya* **1966**, *7*, 861.
(62) Holmes, H. F.; Mesmer, R. E. *J. Chem. Thermodyn.* **1983**, *15*, 709.
(63) Ananthaswamy, J.; Atkinson, G. *J. Chem. Eng. Data* **1985**, *30*, 120.
(64) Rogers, P. S. Z.; Pitzer, K. S. *J. Phys. Chem.* **1981**, *85*, 2886.
(65) Pitzer, K. S.; Peiper, J. C.; Bisey, R. H. *J. Phys. Chem. Ref. Data* **1984**, *13*, 1.
(66) Culberson, C. H.; Latham, G.; Bates, R. G. *J. Phys. Chem.* **1978**, *82*, 2693.
(67) Krumgalz, B. S.; Millero, F. J. *Marine Chem.* **1983**, *13*, 127.
(68) Lilley, T. H.; Briggs, C. C. *Proc. R. Soc. London* **1976**, *349A*, 355.
(69) Nakayama, F. S.; Rasnik, B. A. *Anal. Chem.* **1967**, *39*, 1022.
(70) Lu, C. H.; Fabuss, B. M. *Ind. Eng. Chem.* Process Des. Dev. **1968**, *7*, 206.

Received for review October 24, 1989. Accepted April 9, 1990. This research was supported by a consortium of 11 major oil production and service companies.

Inverse Gas Chromatography. 7. Polymer–Solvent Interactions of Hydrocarbon Polymers

Qiangguo Du,[†] **Paul Hattam,**[‡] **and Petr Munk***

Department of Chemistry and Center for Polymer Research, The University of Texas at Austin, Austin, Texas 78712

Inverse gas chromatography has been used to generate a comprehensive set of interaction data for 9 hydrocarbon polymers and 43 solvents. The solvents cover a wide range of different chemical families, and the polymers possess increasing amounts of backbone substitution. For each polymer–solvent system, the specific retention volume, the Flory–Huggins interaction coefficient, χ_{12}, and the excess cohesive energy per unit volume, B_{12}, are presented.

Introduction

Inverse gas chromatography (IGC) has been used for the determination of polymer–solvent interaction coefficients since Guillet and co-workers, some 2 decades ago, introduced a method of data analysis based on the use of weight fraction activity coefficients (*1–3*). The IGC technique is relatively rapid, and when appropriate precautions are taken (*4*), it is rather precise. Yet, as far as we are aware, no systematic study has been made to measure the interaction coefficients of many solvents (probes) with a large number of polymers. Although a large number of studies have been made, for example, refs 5–13, there is little consistency between the experimental conditions or probes used, which makes the comparison of results difficult. A systematic study of numerous polymers and their interaction with a large number of probes would help clarify the relations between the chemical structure of the polymer and the probe and their interaction behavior. (Of course, the added advantage of such a comprehensive study is the internal consistency of the results.) This paper is intended as a first step in that direction.

Theory

By combination of standard chromatographic equations (*14*) with the Flory–Huggins theory of polymer solutions (*15*), extended to infinite dilution (*16*), the Flory–Huggins interaction coefficient χ_{12} may be obtained as

$$\chi_{12} = \ln (RTv_2/V_g p_1^\circ V_1) - 1 + V_1/M_2 v_2 - (B_{11} - V_1)p_1^\circ/RT \quad (1)$$

V_g is the specific retention volume of the probe, V_1 is its molar volume, and B_{11} and p_1° are the probe's second virial coefficient in the gas phase and the saturated vapor pressure of the pure probe, respectively. M_2 is the molecular weight of the polymer, and v_2 is its specific volume. R is the gas constant, and T is the temperature of the column. The specific retention volume is determined as

$$V_g = j(t_p - t_m)F/w \quad (2)$$

where w is the weight of the polymer on the column and F is the carrier gas flow rate at the column temperature and at the

---

[†] Present address: Department of Materials Science, Fudan University, Shanghai 200433, People's Republic of China.

[‡] Present address: 3M Industrial and Electronic Sector Research Laboratory, 3M Center, St. Paul, MN 55144.

0021-9568/90/1735-0367$02.50/0 © 1990 American Chemical Society